REHABILITATION BIOMECHANICS

Final Project

Table of Contents

0 Introduction

This project is based on the data collected in an experiment that was conducted in the Bio-robotics and Biomechanics Lab (BRML) at the Technion. The experiment included one female subject that walked back and forth on a fixed path with various speeds and different shoes. The path included a built-in force plate to measure the forces applied on the ground during a sample step, and a surrounding motion capture system to measure selected joint positions throughout the experiment. Additionally, the stress distribution in the foot a was measured using an insert.

Figure 0.1 – The Pedar measurement system (https://novel.de/products/pedar/)

The data collected from the motion capture system included but not limited to the joints positions throughout the motion in each of the 16 trials. The data collected from the EMG devices included the surface EMG signals at different muscle positions.

The possible measurement errors for the EMG signals include Soft Tissue Artifact (STA) and the effect of placement of the sensors on cloths of the subject. Measurement errors for the motion capture system are limited to the calibration process, and to the sensing system rated sensitivity. Regarding the stress distribution measurements from the Pedar system, the position of the foot with respect to the insert and the possibility of the foot shifting during the motions can introduce errors to the measured data.

1 Gait Analysis

1.1 Gait cycle

a) We calculated the absolute time vector for the devices table according to the formula:

$$t_i = (F_i \cdot 18 + SF_i)/f_s$$

Where F_i is the i-th frame and FS_i is the i-th subframe, and f_s is the sampling rate for the analog devices. For the model table we used this formula as it did not include a subframe.

$$t_i = F_i/f_s$$

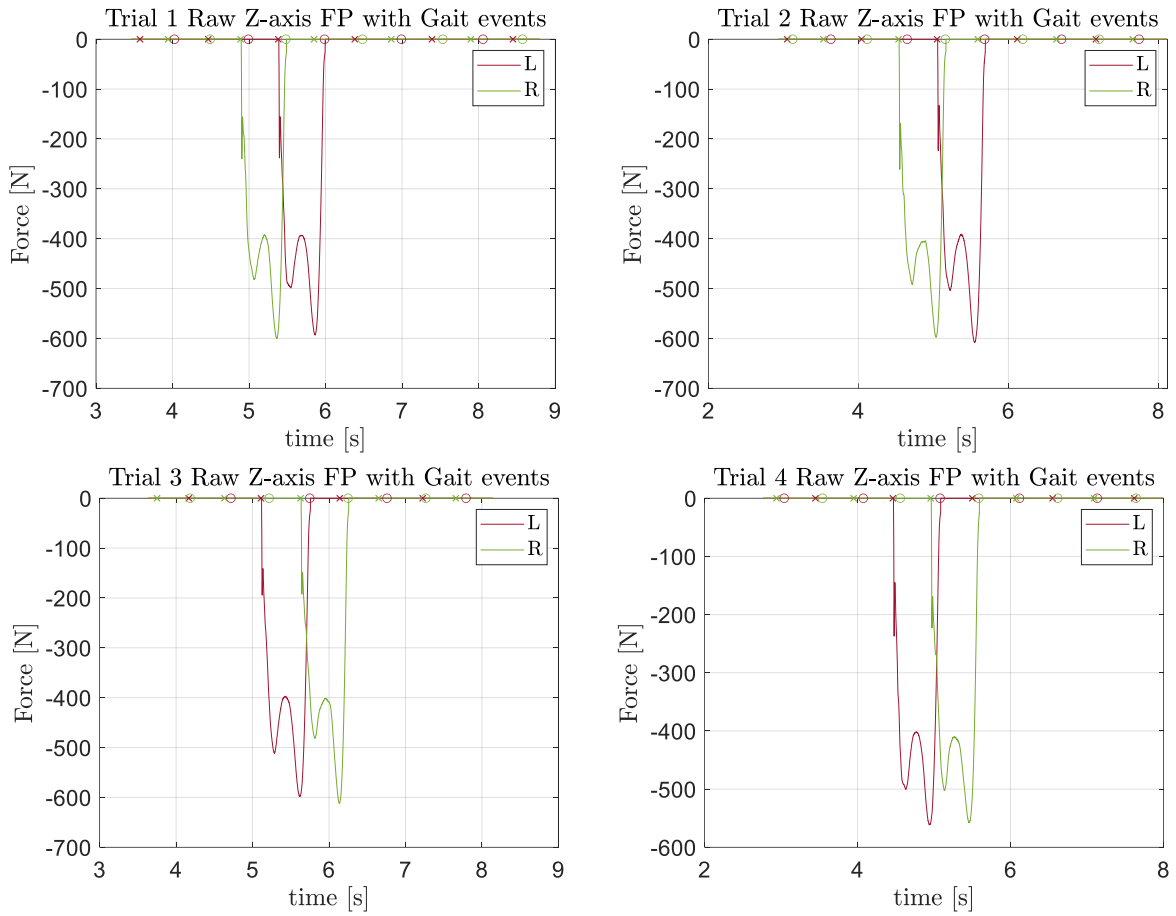

Figure 1.1 - Raw Z axis Force Plate measurements with gait events for Right and Left sides. A foot strike (FS) is given by an "x" and a foot off (FO) is given by an "o" marker.

b) We plotted for each trial (1 to 4) for each side (left and right) the mean pelvic rotations and the standard deviations of the interpolated gait cycles. We used the Acronyms for Flexion/Extension (FE), Adduction/Abduction (AA) and Internal/External Rotation (IER), and in the context of the Pelvis, FE is Pelvic tilt, AA is Pelvic obliquity and IER is the Pelvic rotation. As previously, we used the red color for the left side and the green color for the right side.

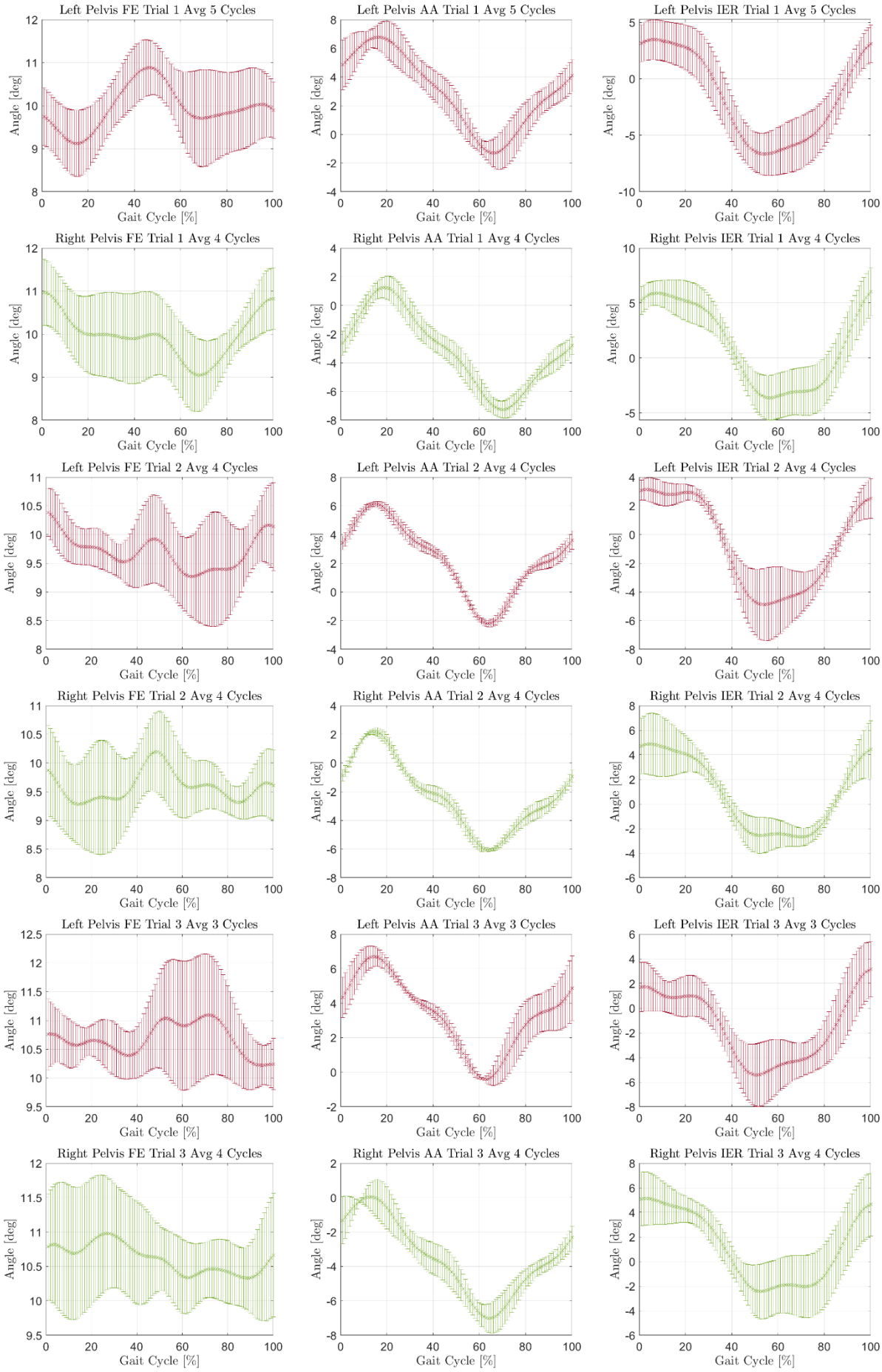
Left Pelvis FE Trial 1 Avg 5 Cycles
Left Pelvis AA Trial 1 Avg 5 Cycles
Left Pelvis IER Trial 1 Avg 5 Cycles
Right Pelvis FE Trial 1 Avg 4 Cycles
Right Pelvis AA Trial 1 Avg 4 Cycles
Right Pelvis IER Trial 1 Avg 4 Cycles
Left Pelvis FE Trial 2 Avg 4 Cycles
Left Pelvis AA Trial 2 Avg 4 Cycles
Left Pelvis IER Trial 2 Avg 4 Cycles
Right Pelvis FE Trial 2 Avg 4 Cycles
Right Pelvis AA Trial 2 Avg 4 Cycles
Right Pelvis IER Trial 2 Avg 4 Cycles
Left Pelvis FE Trial 3 Avg 3 Cycles
Left Pelvis AA Trial 3 Avg 3 Cycles
Left Pelvis IER Trial 3 Avg 3 Cycles
Right Pelvis FE Trial 3 Avg 4 Cycles
Right Pelvis AA Trial 3 Avg 4 Cycles
Right Pelvis IER Trial 3 Avg 4 Cycles
Angle [deg]
Gait Cycle [%]

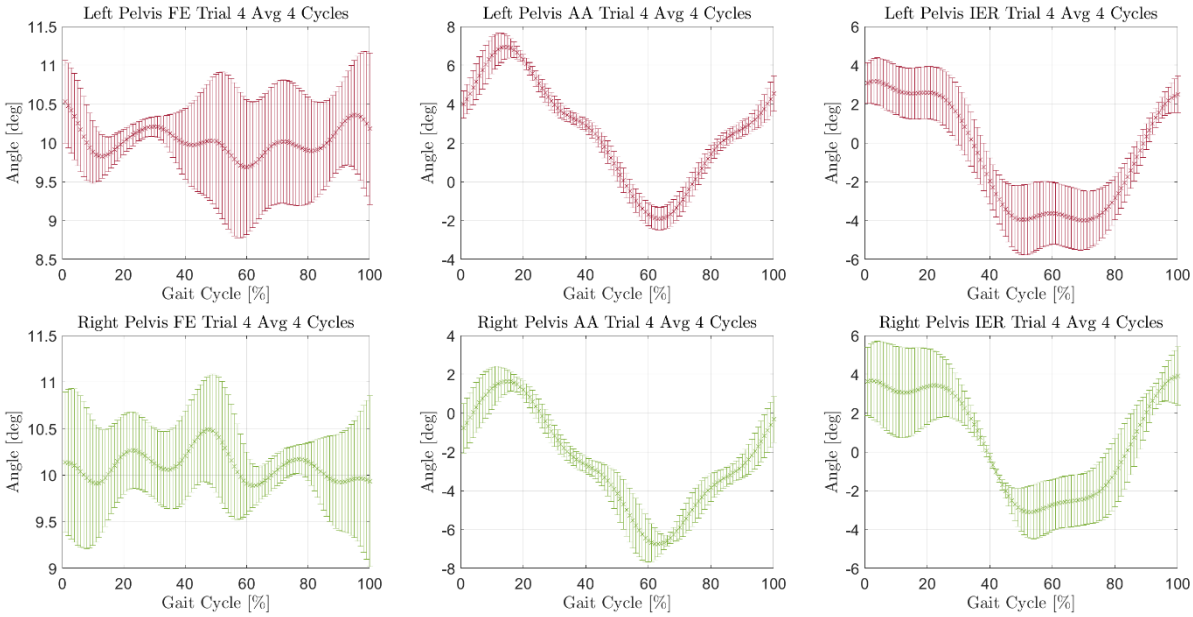

Figure 1.2 - The average and error of Pelvis rotations for each trial for left and right side throughout the Gait cycle.

c) We compared the results with Pelvic biomechanical angles during normal speed gait for females using the studies [1], [2] using the following results.
For qualitative reasons we observed the anatomical angles plots vs the gait cycle percentage as given in [1]. The pelvic rotation starts at some positive angle, then within half of the cycle it falls to a minimum and rises back up to the start of the next gait cycle. This was apparent in all our average results in Figure 1.1. The pelvic Obliquity start at nil and increases, then it is symmetrically matched below. Although this result agrees qualitatively, in our Right pelvis values the range is nearly half of the Left side, which suggests that either the subject has an asymmetric gait or that our analysis was incorrect. The left side falls within the appropriate range when compared to the study. Finally, the Pelvic tilt is inconclusive because of the large error range, however it does show significantly larger values (~10 degrees) as opposed to 4 degrees in the study. This may be due to an inherent bias in the motion capture sensing system or its angle estimation.

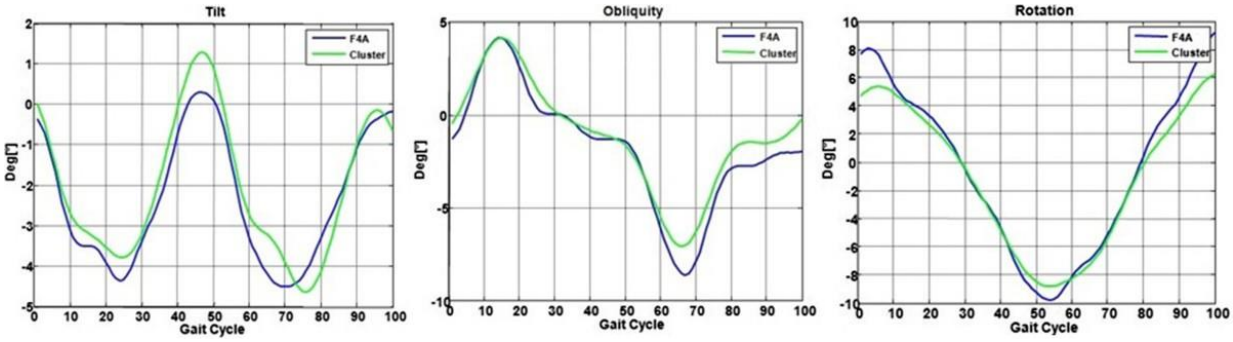

In addition, we looked at the normal values given in the table below in [2]. We found that for medium speed for Females, a typical pelvic tilt can reach ~10 degrees within two standard deviations. We also saw that the pelvic obliquity is slightly higher than given in our results but all within a standard deviation.

Table 2. Spatiotemporal outcomes according to sex and speed levels.

	Males (SD)	Females (SD)	Mean Differences (min–max)
		Slow Speed	
Symmetry index (%)	99.04 (0.69)	99.37 (0.34)	−0.33 (−0.80–0.14)
Cadence (p/m)	170.1 (9.7)	171.9 (15.5)	−1.76 (−9.56–6.04)
Stride time (s)	0.70 (0.04)	0.69 (0.06)	0.01 (−0.03 a −0.04)
Stride length (m)	1.81 (0.12)	1.30 (0.14)	0.22 (0.08–0.35)
Pelvic tilt (°)	6.27 (1.70)	6.26 (2.40)	−0.01 (−1.37–1.77)
Pelvic rotation (°)	10.64 (2.47) **	13.21 (2.98) **	−2.57 (−5.09 a −0.05)
Pelvic obliquity (°)	9.27 (2.53)	8.11 (1.34)	1.16 (−1.18–2.51)
		Medium Speed	
Symmetry index (%)	99.43 (0.44)	98.89 (0.73)	0.55 * (0.07–1.03)
Cadence (p/m)	173.0 (10.4)	172.2 (10)	7.81 (−7.02–8.59)
Stride time (s)	0.67 (0.05)	0.69 (0.04)	−0.01 (−0.04–0.02)
Stride length (m)	2.02 (0.23)	1.84 (0.10)	0.18 (0.06–0.31)
Pelvic tilt (°)	5.92 (2.46)	6.57 (2.58)	0.65 (−1.45–1.65)
Pelvic rotation (°)	9.96 (3.76) **	15.74 (3.99) **	−5.78 (−8.26 a −3.30)
Pelvic obliquity (°)	7.84 (2.16)	9.64 (1.77)	−1.80 *(−3.12 a −0.47)
		Fast Speed	
Symmetry index (%)	98.62 (0.82)	98.99 (0.73)	−0.37 (−0.81–0.08)
Cadence (p/m)	171.3 (9.39)	173.5 (10)	−2.117 (−9.47–5.24)
Stride time (s)	0.70 (0.04)	0.69 (0.24)	0.01 (−0.02–0.04)
Stride length (m)	2.47 (0.27)	2.14 (0.14)	0.33 (0.21–0.45)
Pelvic tilt (°)	6.50 (2.00)	7.36 (2.22)	0.86 (−2.38–0.58)
Pelvic rotation (°)	13.60 (3.68) **	16.13 (3.42) **	−2.53 (−4.91 a −0.16)
Pelvic obliquity (°)	8.75 (1.44)	7.81 (1.99)	0.95 (−2.23–0.34)

* Significant difference $p < 0.025$ between groups (Males–Females) ** Significant differences $p < 0.05$ within groups (sex–speed levels).

1.2 Ground Reaction Forces

a) We calculated the Total GRF for each walking condition at normal speed for right leg only and resulted with the following plots.

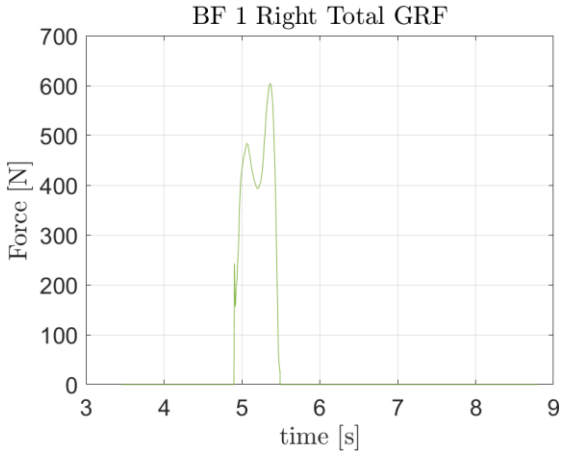
BF 1 Right Total GRF
Force [N]
time [s]

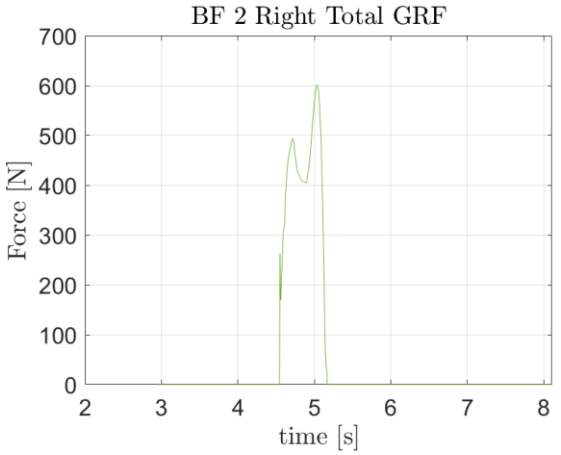
BF 2 Right Total GRF
Force [N]
time [s]

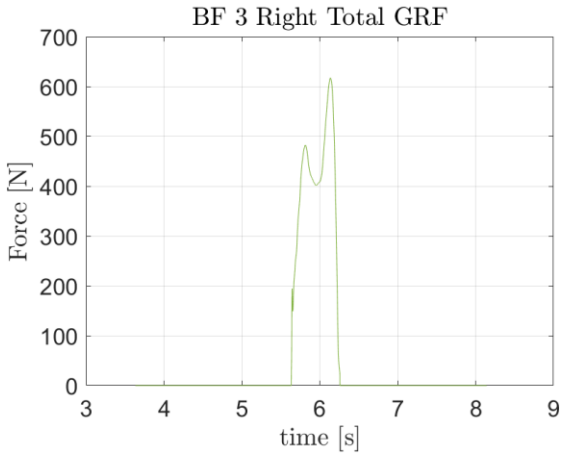
BF 3 Right Total GRF
Force [N]
time [s]

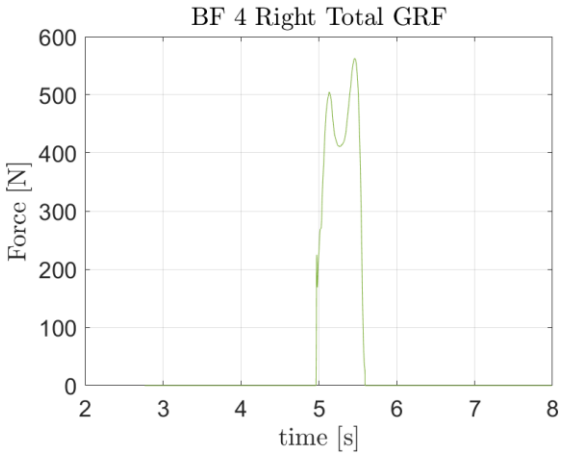
BF 4 Right Total GRF
Force [N]
time [s]

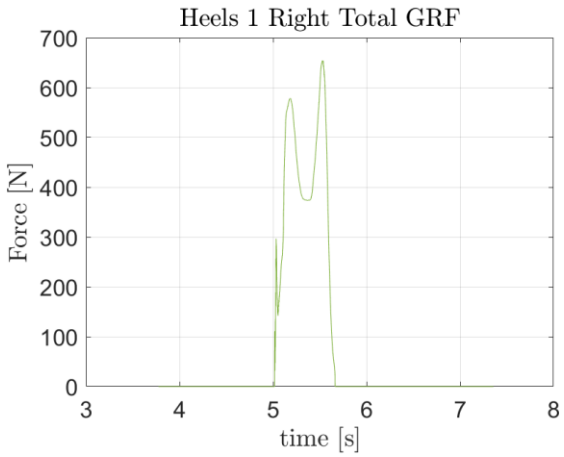
Heels 1 Right Total GRF
Force [N]
time [s]

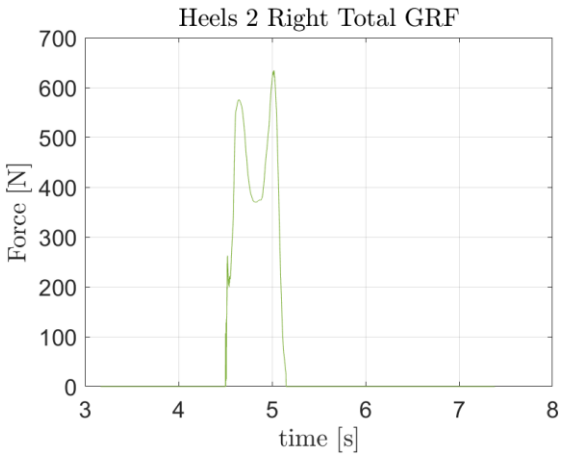
Heels 2 Right Total GRF
Force [N]
time [s]

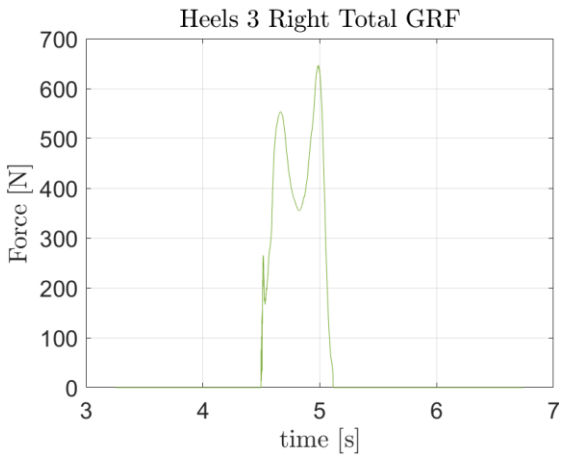
Heels 3 Right Total GRF
Force [N]
time [s]

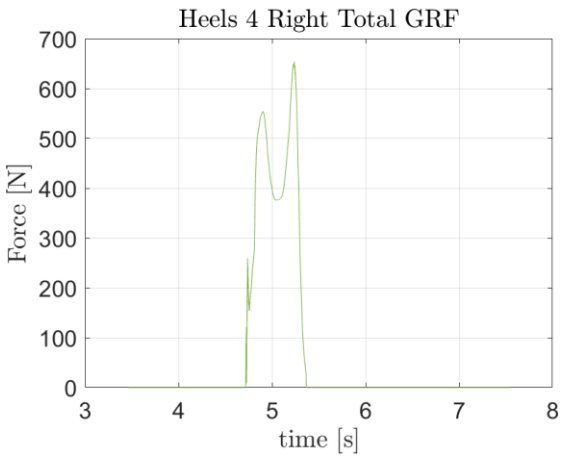
Heels 4 Right Total GRF
Force [N]
time [s]

Figure 1.3 – Total GRF for the Right foot during the normal speed for Barefoot and heels condtions.

b) We can see that for the Heels condition the peak value rises above the peak value for the barefoot condition. This can be because of the extra weight added to the subject when adding a heel shoe, or it can also be due to the larger impulse that the heels generate on the ground as opposed to the barefoot condition because the heels have a smaller surface area touching the ground yet must generate similar forces.

1.3 Estimation of spatiotemporal parameters

a) We chose to use the Right Ankle (RANK) marker as a measure for the distance traveled within each gait cycle. We took each measurement of the lab coordinate system and found its interpolated gait cycle data. Then we calculated numerically the velocity of the Ankle in between each two interpolated samples and calculated the mean value of the entire gait cycle velocity for each trial per whole gait cycle. The following table summarizes the estimated average velocity in meters per second. The rows represent each trial, and the columns represent each whole gait cycle found. Cases of zero value occurred when the Foot strike event was not properly found within a require tolerance (We used the “ismembertol” function in MATLAB)

	Gait Cycle 1	Gait Cycle 2	Gait Cycle 3	Gait Cycle 4
BF fast 1	1.48	1.72	1.66	
BF fast 2	1.54	1.83		
BF fast 3	1.56	1.66		
BF fast 4	1.93	1.83	1.79	
BF normal 1	1.26	1.25	1.26	1.14
BF normal 2	1.23	1.23	1.16	1.07
BF normal 3	1.35	1.33	1.42	1.35
BF normal 4	1.17	1.17	1.23	1.11
Heels normal 1	1.31	1.30	1.36	
Heels normal 2	1.32	1.34	1.34	
Heels normal 3	1.34	1.39	1.36	
Heels normal 4	1.30	1.36	1.32	
Heels slow 1	0.97	0.95	0.96	
Heels slow 2	1.03	1.048	0.94	0.90
Heels slow 3	0.97	1.08	1.10	
Heels slow 4	1.01	0.99	1.00	

2 Electromyography

2.1 EMG Signal Processing

We computed the EMG signals according to the following steps:

1) First, we found the Power Spectrum of the signals and chose the appropriate Band Pass filtering frequencies. We included an example plot for the first signal power spectrum and the cut off frequencies.

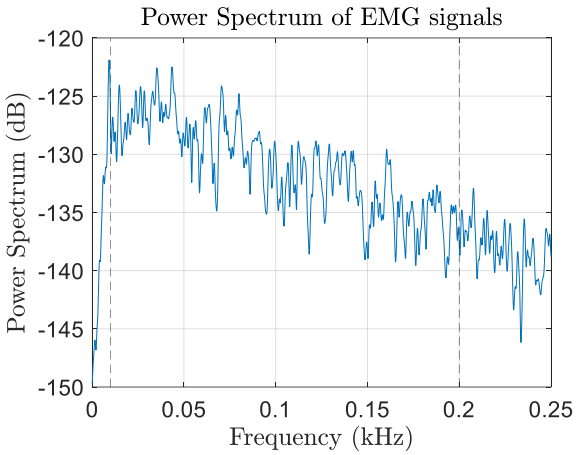

Figure 2.1 - Power spectrum example of EMG1 signal during barefoot condition in normal speed (trial 1) with cut off frequencies presented in dashed vertical lines. We disregarded the higher frequency data by chooosing a limit of 250 Hz for the plot, however the power spectrum is existant in higher frequencies.

2) We used a low pass frequency of 200 Hz and a high pass frequency of 10 Hz to construct a Butterworth Band Pass filter and chose a 4^{th} order one.
3) We removed the bias of the signal and applied the BPF and then applied a full wave rectification using the absolute value.
4) We calculated a moving average with a window of 50 values and found the envelope.
5) We applied these steps for all 8 trials for both sensors and plotted the raw EMG signal, the rectified filtered signal and its RMS envelope as an area chart.
6) Additionally, we added to each plot the gait events of FS as a solid line (-) and FO as a dashed line (--) with a color according to the convention used above for Left and Right.

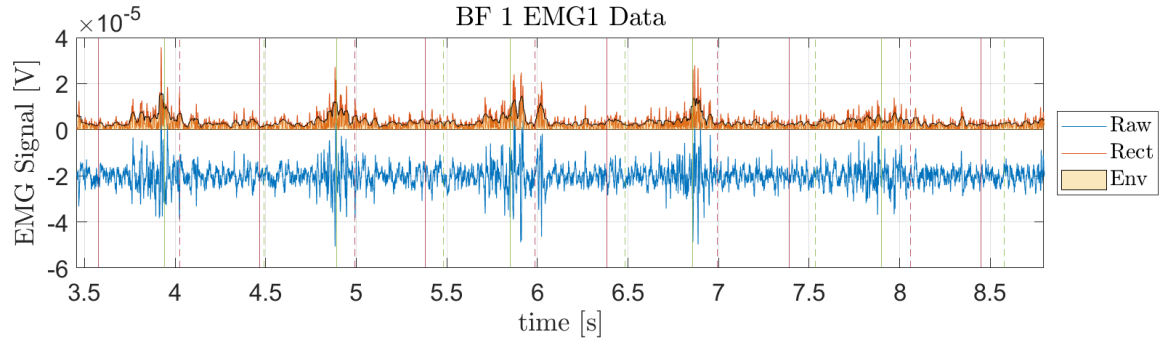
BF 1 EMG1 Data
×10^-5
EMG Signal [V]
time [s]
Raw
Rect
Env

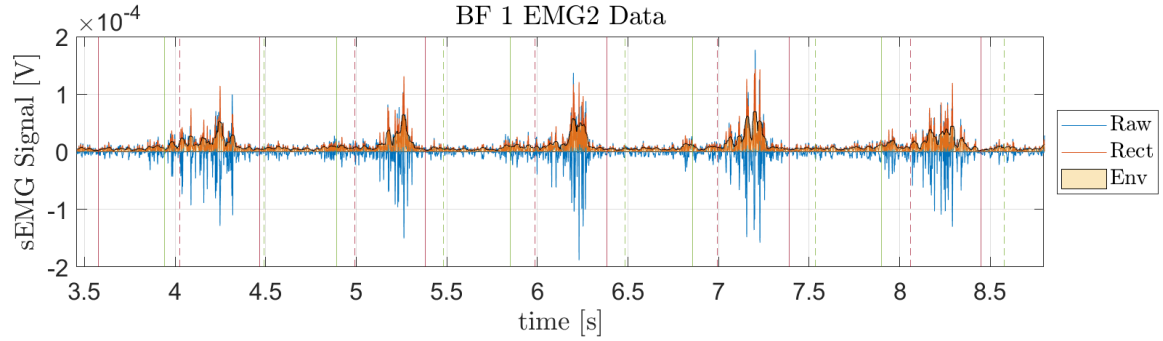
BF 1 EMG2 Data
×10^-4
sEMG Signal [V]
time [s]
Raw
Rect
Env

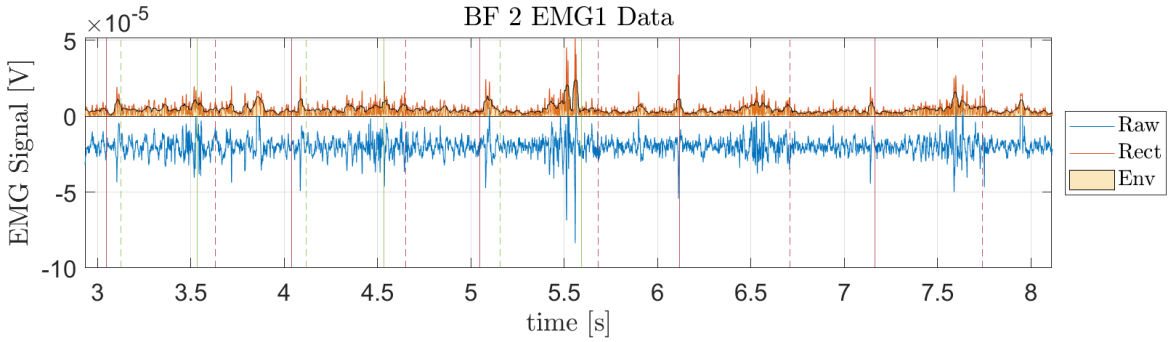
BF 2 EMG1 Data
×10^-5
EMG Signal [V]
time [s]
Raw
Rect
Env

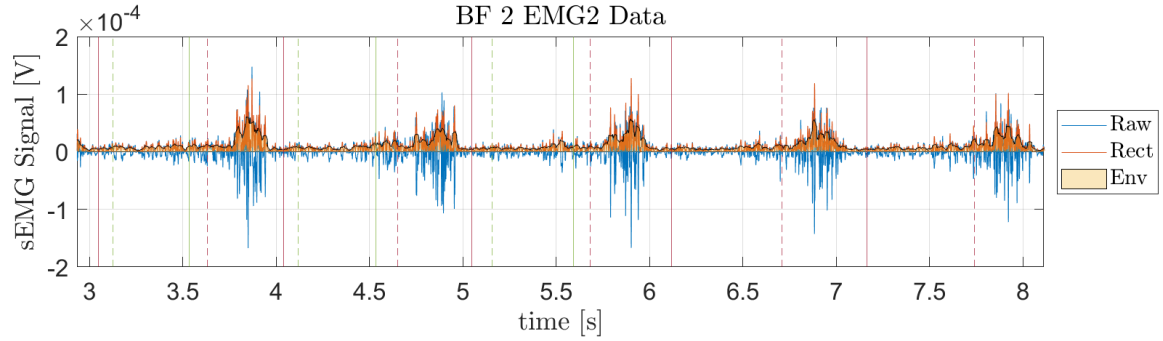
BF 2 EMG2 Data
×10^-4
sEMG Signal [V]
time [s]
Raw
Rect
Env

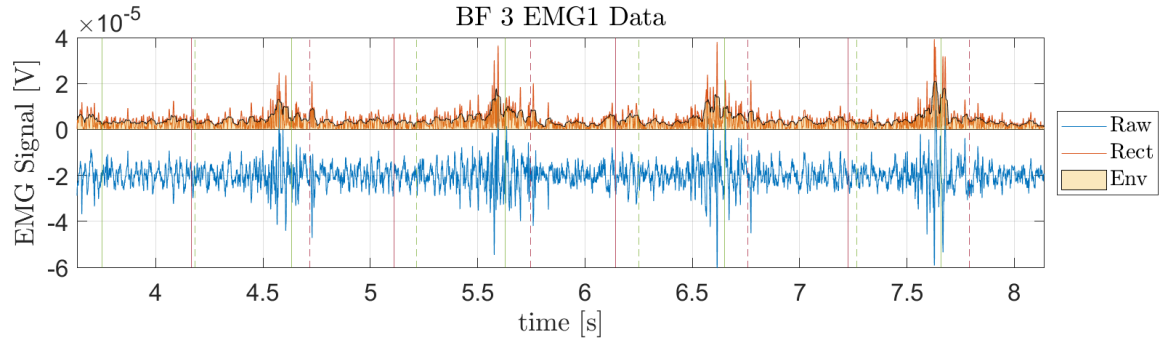
BF 3 EMG1 Data
×10^-5
EMG Signal [V]
time [s]
Raw
Rect
Env

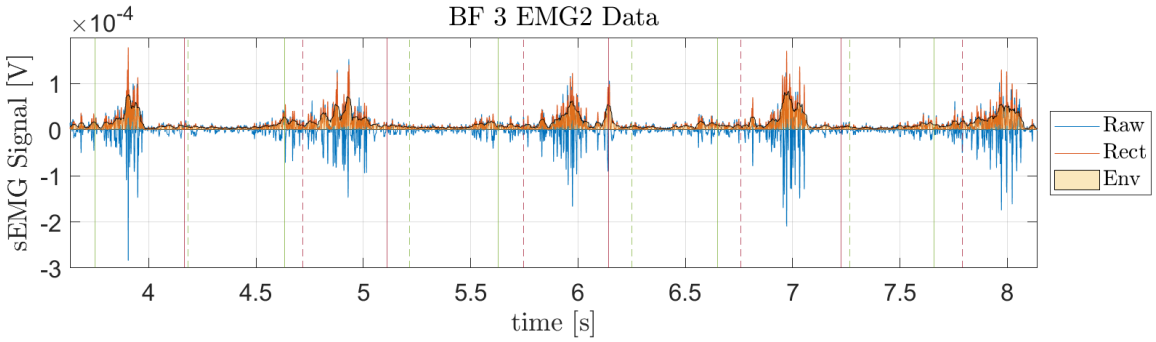
BF 3 EMG2 Data
×10^-4
sEMG Signal [V]
time [s]
Raw
Rect
Env

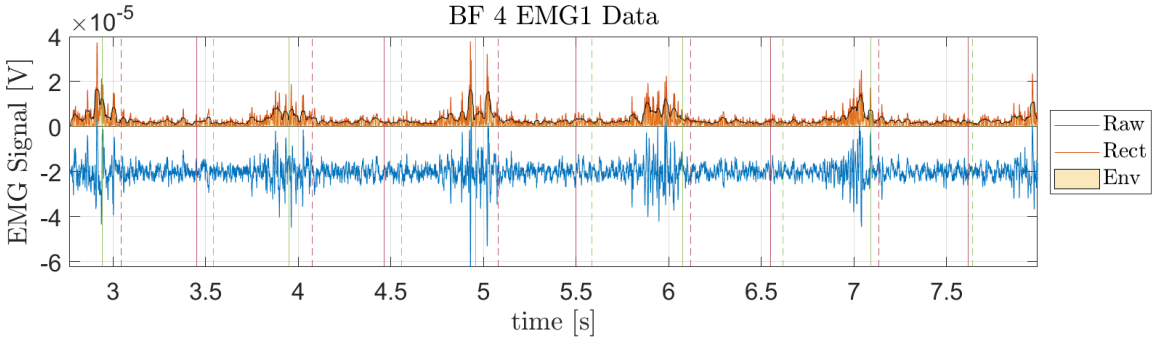
BF 4 EMG1 Data
×10^-5
EMG Signal [V]
time [s]
Raw
Rect
Env

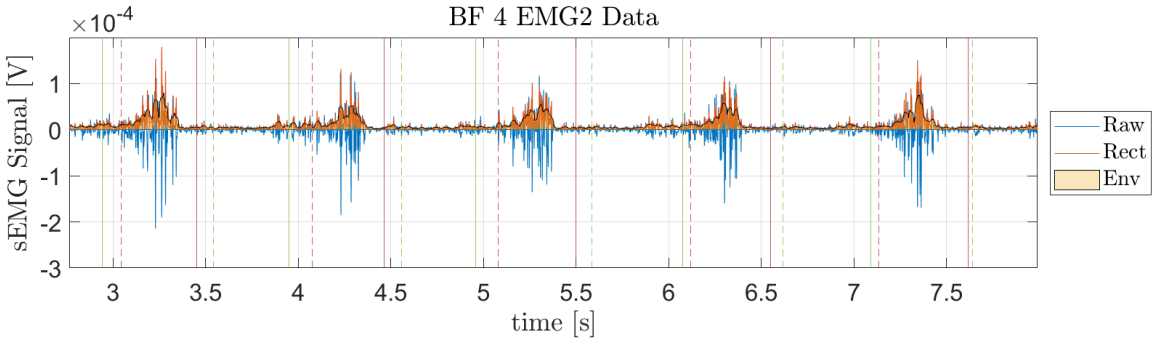
BF 4 EMG2 Data
×10^-4
sEMG Signal [V]
time [s]
Raw
Rect
Env

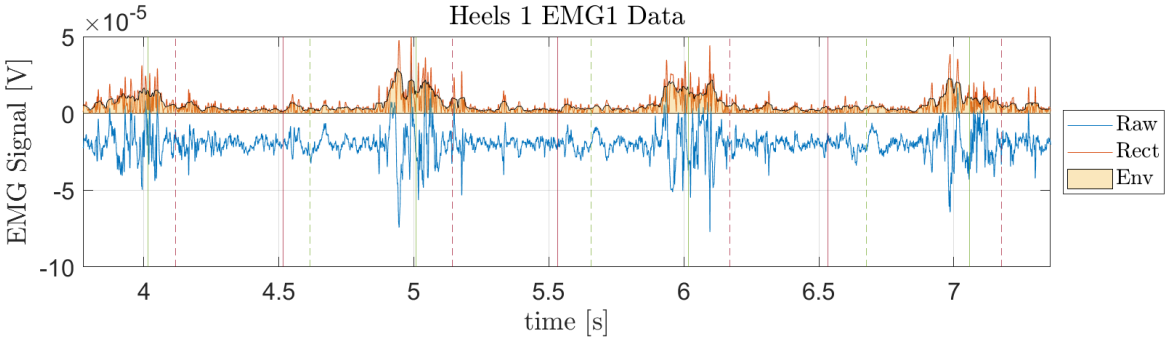
Heels 1 EMG1 Data
×10^-5
EMG Signal [V]
time [s]
Raw
Rect
Env

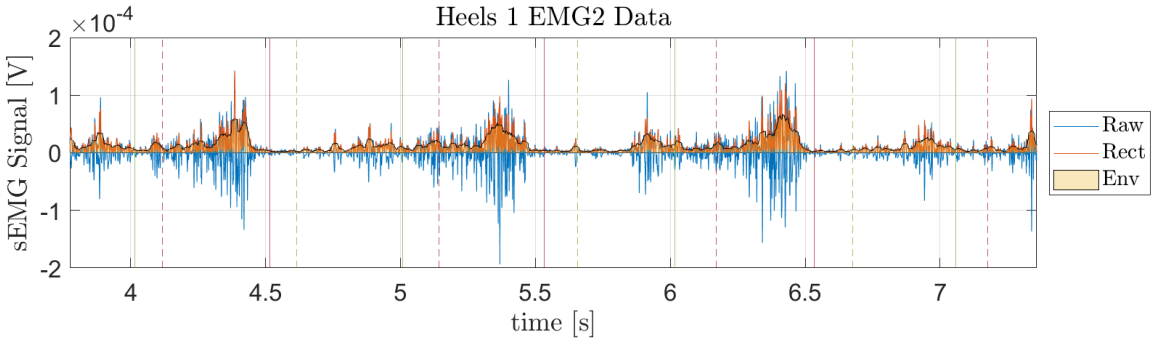
Heels 1 EMG2 Data
×10^-4
sEMG Signal [V]
time [s]
Raw
Rect
Env

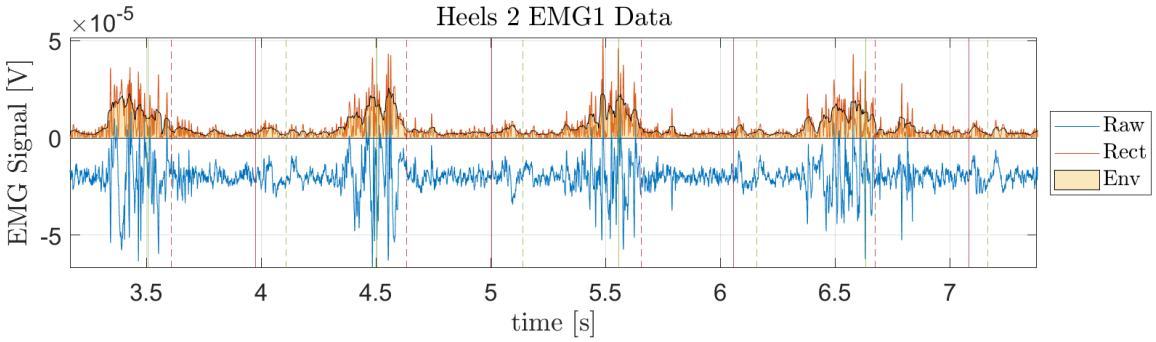
Heels 2 EMG1 Data
×10^-5
EMG Signal [V]
time [s]
Raw
Rect
Env

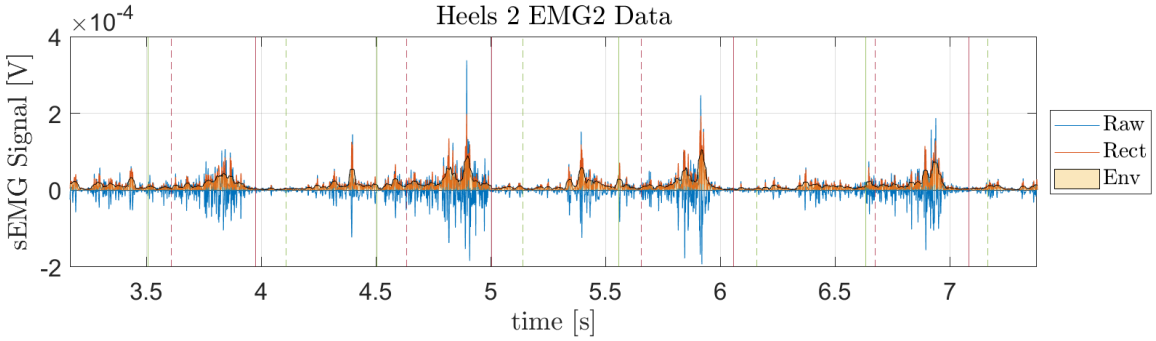
Heels 2 EMG2 Data
×10^-4
sEMG Signal [V]
time [s]
Raw
Rect
Env

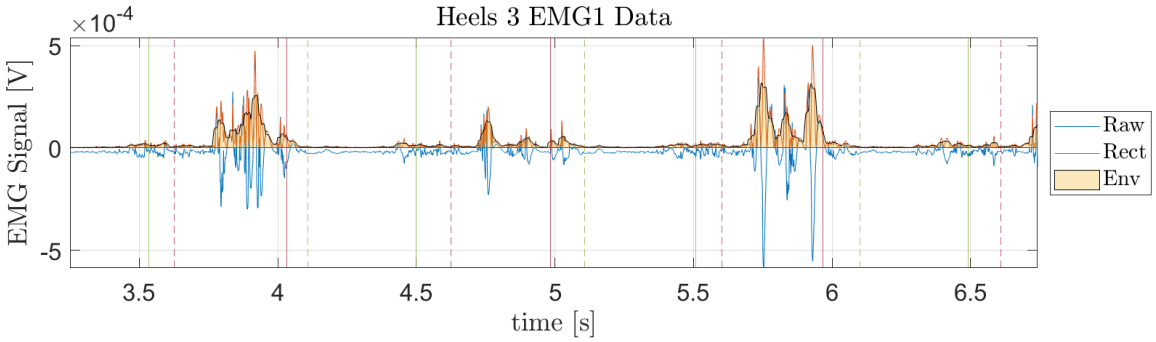
Heels 3 EMG1 Data
×10^-4
EMG Signal [V]
time [s]
Raw
Rect
Env

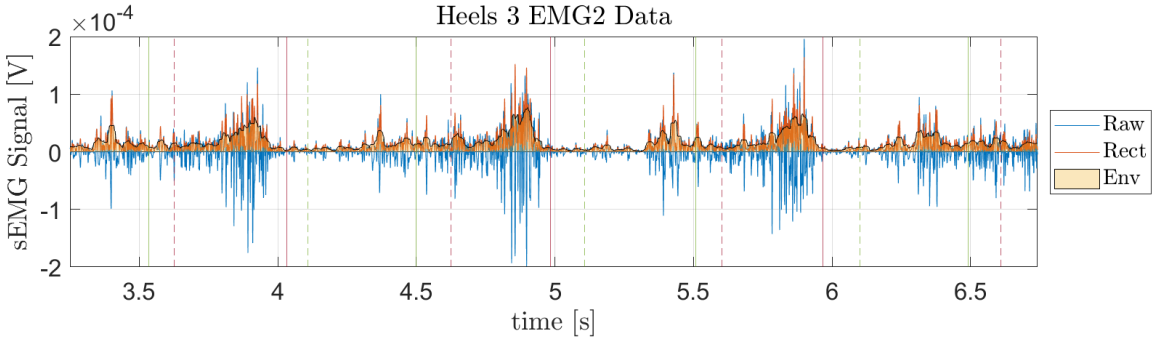
Heels 3 EMG2 Data
×10^-4
sEMG Signal [V]
time [s]
Raw
Rect
Env

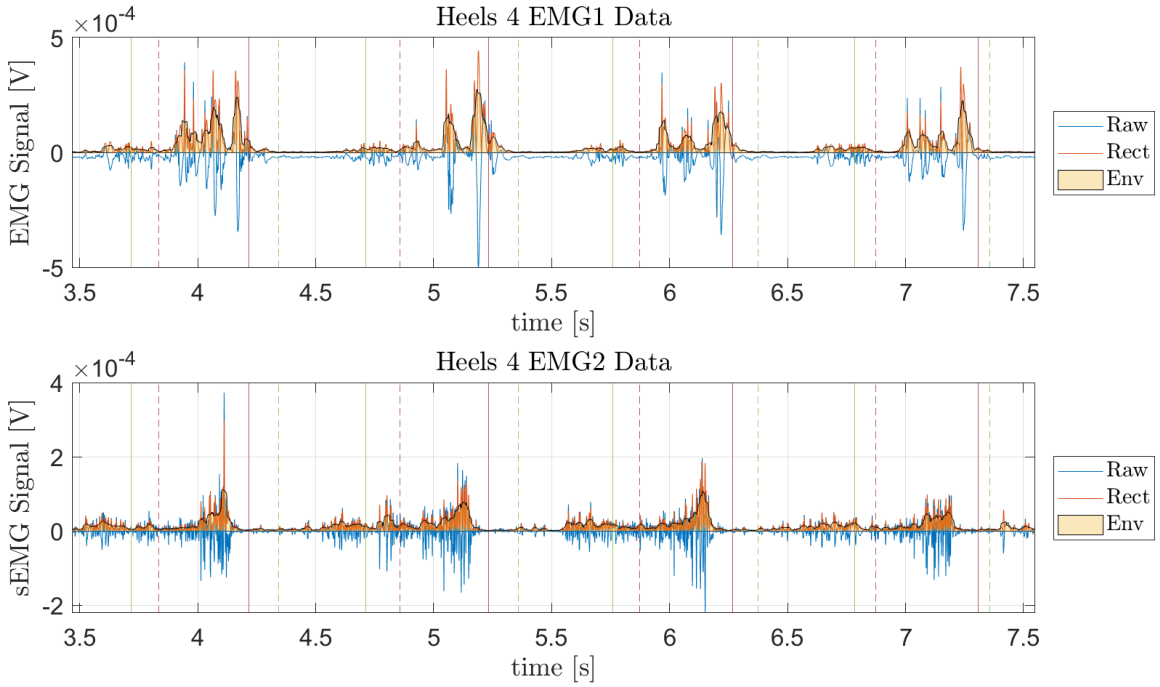

Figure 2.2 - EMG signals for both sensors for all trials in normal condition. Each plot includes the raw EMG signals, the rectified signal (filtered) and the RMS envelope signal. in addition, the gait events for both the left and right FS and FO are shown in vertical lines.

As shown above, the Heels condition display larger peaks in the rectified signals with respect to the Barefoot condition. In addition, the envelope signal is more spread out in the Barefoot condition which suggests that the muscle activity for the barefoot condition is lower in magnitude but occurs for a longer duration.

For the Heels condition, the activity starts toward the middle of the gait cycle and ends slightly before it ends. (Consider FS to FS as a gait cycle of the Left side events shown in red). For the Barefoot condition the activity is like the previous phenomenon for the second sensor (EMG2), but for the first sensor (EMG1) the activity seems to be reversed to the right-side gait cycles (FS are shown in green solid vertical lines).

2.2 Identification of muscles using EMG signals

We used the study [3] as a reference for the EMG signals during a gait cycle. The figure we used as reference is given in Figure 2.3. It is shown that the LG muscle activity during the gait cycle is concentrated only in one part of the cycle, whereas the RF activity occurs twice in the cycle and for a longer duration. This suggests that the EMG1 sensor (i.e., device 1) was place on the LG muscle, because its peak activity occurs in one location during the cycle (20%-50%). It follows that the EMG2 sensor (i.e., device 5) was most likely placed on the RF muscle, because the activity was concentrated in both points during the gait cycle, including the Foot Strike event and in between Foot strikes.

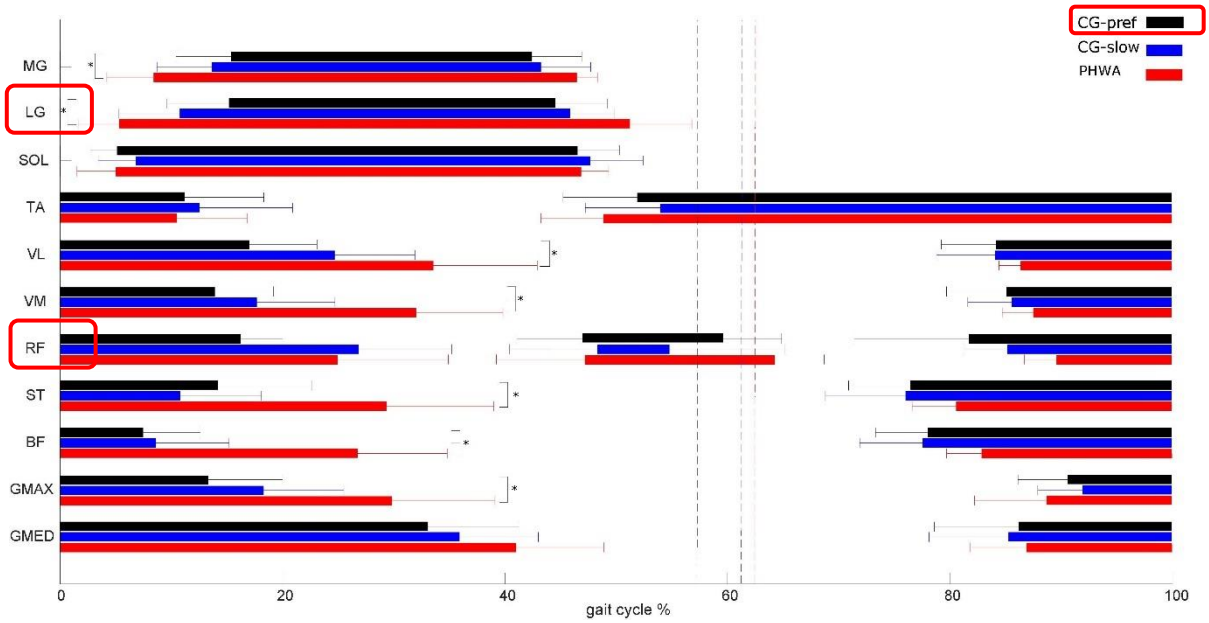

Figure 2.3 - A figure (#7) taken from study [3] to classify activity of LG and RF muscles during normal gait cycle.

3 Pedobarography

3.1 Sampling rate

The sampling rate of the Pedar device is simply given by the inverse time difference between two consecutive samples. Therefore, $f_s = \frac{1}{t_2 - t_1} = 100[Hz]$.

3.2 Stance Phases

First, we plotted the forces of all trials over time to understand the meaning of the stance phases.

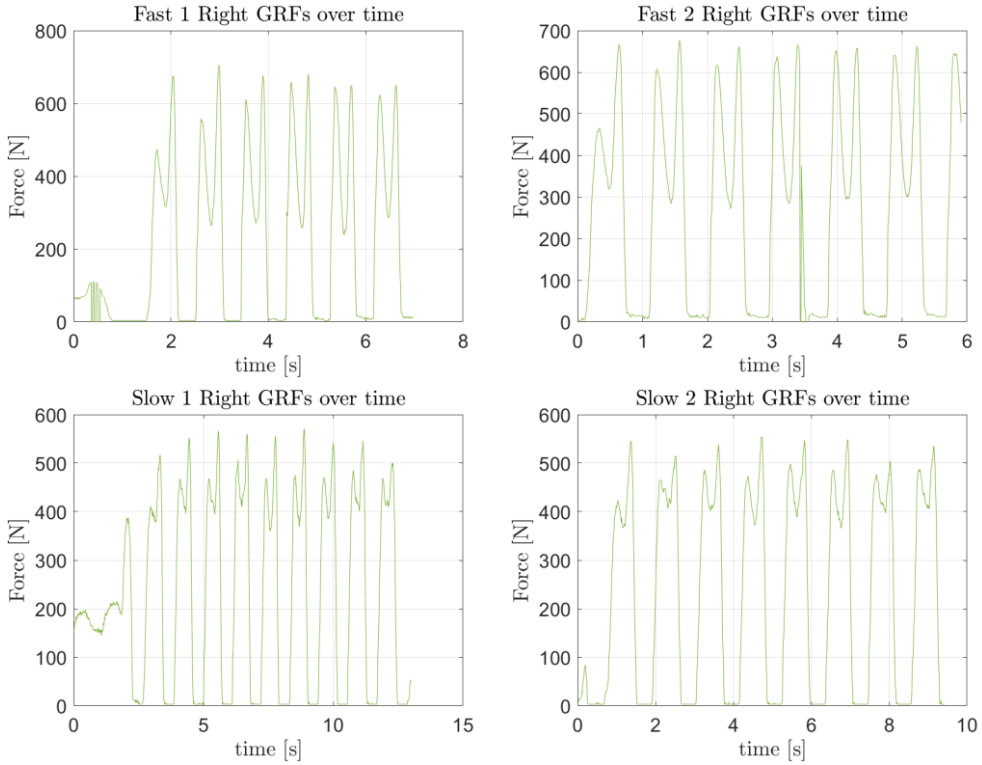

We observed that the GRF repeatedly reaches zero, which we conclude it to be the point in time where the foot is above the ground. We chose the stance phase to start when the GRF increases from a small value above a certain threshold, and to end when it decreases below the same threshold. To automatically find these times we built a custom function that find the envelope of the signal using an RMS as used in the EMG analysis. Then we looked for indexes that change from low to high or from high to low. The resulting indexes using a threshold of 100 [N] and a window of 10 samples is given by:

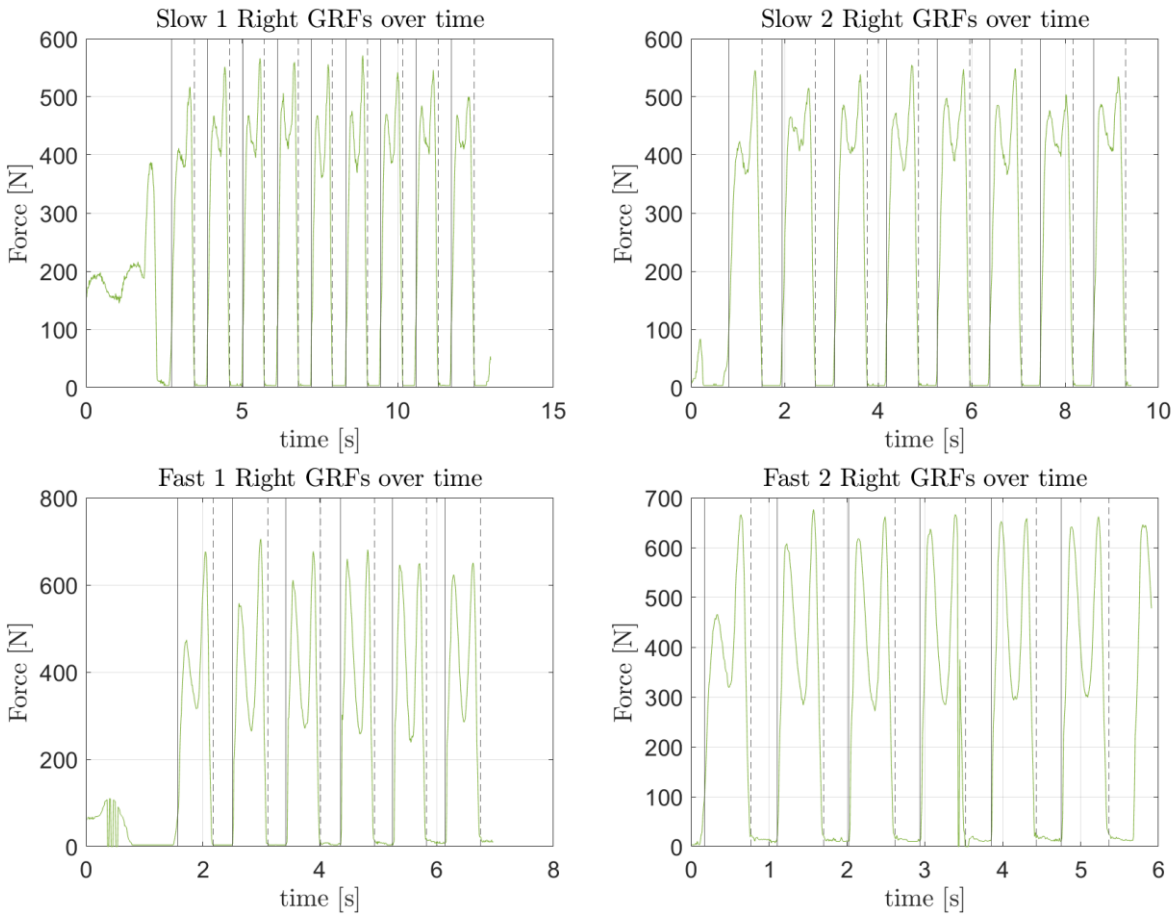

Figure 3.1 - The Stance Phases start (solid line (-)) and end (dashed line (--)) times for all trials of the Right foot.

3.3 Optional Question

3.4 COP plots

We plotted the trajectory of the COP in all Stance Phases (SP) per each trial as given in the figure below.

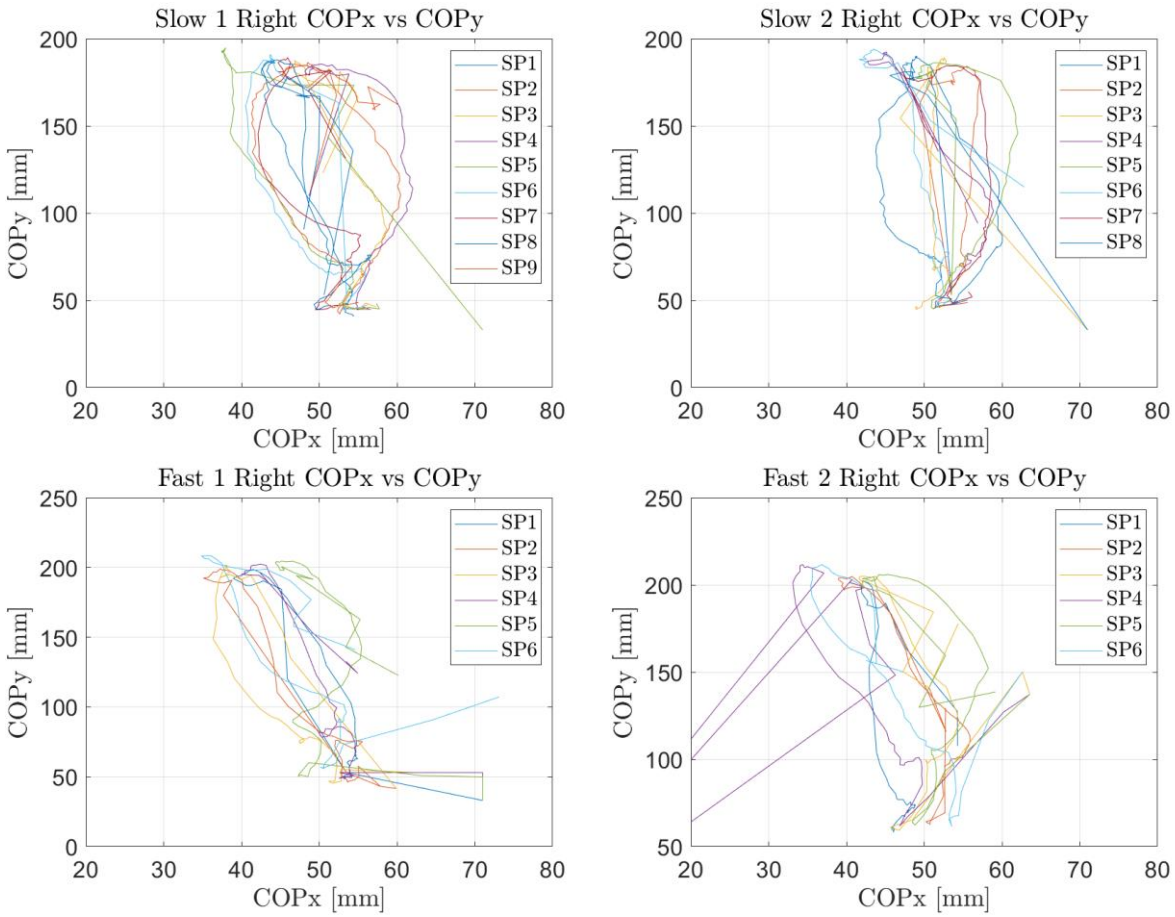

Figure 3.2 - COP trajectory for each Stance Phase for all trials.

4 Bibliography

[1] F. Buganè, M. G. Benedetti, V. D'Angeli, and A. Leardini, "Estimation of pelvis kinematics in level walking based on a single inertial sensor positioned close to the sacrum: Validation on healthy subjects with stereophotogrammetric system," *Biomed Eng Online*, vol. 13, no. 1, pp. 1–15, Oct. 2014, doi: 10.1186/1475-925X-13-146/TABLES/6.

[2] S. Perpiñá-Martínez, M. D. Arguisuelas-Martínez, B. Pérez-Domínguez, I. Nacher-Moltó, and J. Martínez-Gramage, "Differences between Sexes and Speed Levels in Pelvic 3D Kinematic Patterns during Running Using an Inertial Measurement Unit (IMU)," *Int J Environ Res Public Health*, vol. 20, no. 4, Feb. 2023, doi: 10.3390/IJERPH20043631.

[3] C. Cruz-Montecinos, S. Pérez-Alenda, F. Querol, M. Cerda, and H. Maas, "Changes in Muscle Activity Patterns and Joint Kinematics During Gait in Hemophilic Arthropathy," *Front Physiol*, vol. 10, p. 489423, Jan. 2020, doi: 10.3389/FPHYS.2019.01575/BIBTEX.